electronics

MDPI

Article

Self-Healing Fiber Bragg Grating Sensor System Using Free-Space Optics Link and Machine Learning for Enhancing Temperature Measurement

Michael Augustine Arockiyadoss [1], Amare Mulatie Dehnaw [1], Yibeltal Chanie Manie [1], Stotaw Talbachew Hayle [2], Cheng-Kai Yao [1], Chun-Hsiang Peng [1], Pradeep Kumar [1] and Peng-Chun Peng [1,*]

[1] Department of Electro-Optical Engineering, National Taipei University of Technology, Taipei 10608, Taiwan; t111659402@ntut.edu.tw (M.A.A.); amare.mulatie@ntut.edu.tw (A.M.D.); yibeltal_chanie@mail.ntut.edu.tw (Y.C.M.); t109658093@ntut.org.tw (C.-K.Y.); t111658059@ntut.org.tw (C.-H.P.); t111999408@ntut.org.tw (P.K.)

[2] Department of Electrical Engineering and Computer Science, Debre Berhan University, Debre Berhan 445, Ethiopia; stotaw19@dbu.edu.et

* Correspondence: pcpeng@ntut.edu.tw; Tel.: +886-2-2771-2171 (ext. 4671)

Abstract: This research investigates the integration of free-space optics (FSO) with fiber Bragg grating (FBG) sensors in self-healing ring architectures, aiming to improve reliability and signal-to-noise ratio in temperature sensing within sensor systems. The combination of FSO's wireless connectivity and FBG sensors' precision, known for their sensitivity and immunity to electromagnetic interference, is particularly advantageous in demanding environments such as aerospace and structural health monitoring. The self-healing architecture enhances system resilience, automatically compensating for failures to maintain consistent monitoring capabilities. This study emphasizes the use of intensity wavelength division multiplexing (IWDM) to manage the complexities of increasing the multiplexing number of FBG sensors. Challenges arise with the overlapping spectra of FBGs when multiplexing several sensors. To address this, a hybrid approach combining an unsupervised autoencoder (AE) with a convolutional neural network (CNN) is proposed, significantly enhancing the accuracy and efficiency of sensor signal detection. These advancements signify substantial progress in sensor technology, validating the effectiveness of the AE-CNN hybrid model in refining FBG sensor systems and underscoring its potential for robust and reliable applications in critical sectors.

Keywords: fiber Bragg grating sensors; free-space optics; self-healing ring architectures; intensity and wavelength division multiplexing; temperature sensing

Citation: Arockiyadoss, M.A.; Dehnaw, A.M.; Manie, Y.C.; Hayle, S.T.; Yao, C.-K.; Peng, C.-H.; Kumar, P.; Peng, P.-C. Self-Healing Fiber Bragg Grating Sensor System Using Free-Space Optics Link and Machine Learning for Enhancing Temperature Measurement. *Electronics* **2024**, *13*, 1276. https://doi.org/10.3390/electronics13071276

Academic Editors: Elias Stathatos and Spyros N. Yannopoulos

Received: 7 March 2024
Revised: 27 March 2024
Accepted: 28 March 2024
Published: 29 March 2024

1. Introduction

Fiber Bragg grating (FBG) sensors have become a fundamental aspect of modern sensor technology, celebrated for their exceptional sensitivity and immunity to electromagnetic interference. These features are particularly crucial in settings where operational conditions are extreme, and the accuracy of measurements is non-negotiable [1–6]. Leveraging a distinct strain-sensing mechanism, FBG sensors are capable of measuring physical parameters like temperature and strain with unparalleled precision, as demonstrated in environments requiring high-temperature monitoring and structural health applications, including aerospace and nuclear reactors [7,8]. This mechanism functions by monitoring shifts in the peak wavelength of the FBG, which occur in response to variations in external stimuli [9–11]. The wide applicability of these sensors spans across diverse sectors, including structural health monitoring and aerospace engineering [12–15], extending to the detection of vital parameters such as vibration and pressure [16–19].

In the rapidly evolving era of the Internet of Things (IoT), where the combination of sensor systems with transmission technologies is essential for extracting valuable data

from a multitude of objects worldwide, FBG sensors play a preferential role. A notable example is discussed in references [20,21], where the combination of laser-driven optical wireless communication (OWC) with fiber optic sensor systems is specifically tailored for IoT applications. This integration harnesses the robustness of OWC in challenging environments to enable the wireless transmission of sensor signals. At this juncture, it is pertinent to introduce free-space optics (FSO), a technology that is rapidly gaining traction in the field of optical communication [22]. FSO operates by transmitting light through the air to deliver high-speed data connectivity [23]. This technology offers the advantages of fiber optics, such as high bandwidth and speed, without the need for physical cables, becoming particularly relevant in environments where laying physical cables is challenging or impractical [24,25]. Despite its susceptibility to atmospheric conditions such as fog, rain, and dust, which can attenuate the signal and the need for precise alignment between transmitting and receiving units, FSO's capability of rapid deployment and high-bandwidth communication without physical infrastructure makes it invaluable. This is especially true in remote or difficult-to-access areas, complementing the precision and reliability of FBG sensors in comprehensive monitoring solutions, thus enhancing the overall performance and applicability of sensor networks in a wide range of environments. The combination of FSO with FBG sensors, as mentioned in references [26,27], highlights a novel approach in communication technology. FSO's ability to provide wireless connectivity complements the precise sensing capabilities of FBG sensors [28,29], enabling more flexible and robust communication systems, especially in areas where traditional wired connections are not feasible. Coupled with the advantages of fiber sensors, such as real-time, precise, and intelligent monitoring, this integration is particularly beneficial for IoT applications [20]. With their high bandwidth, small size, and resistance to electromagnetic interference, optical fiber sensors are becoming increasingly popular as cost-effective solutions that can sense things in many places without the requirement for electronic components at certain sensor locations [16–19]. A distinctive feature of FBG sensors is their capability in multiplexing scenarios, especially within wavelength division multiplexing (WDM) systems. However, a limitation arises in these systems due to the potential for interference when the reflection spectra of sequential FBGs overlap, restricting the number of sensors that can be effectively multiplexed. To address the multiplexing challenges in FBG sensors, intensity and wavelength division multiplexing (IWDM) was proposed [30–32] as an advanced solution, offering an enhanced approach for managing the intricacies associated with such challenges. In the context of IWDM, the occurrence of overlap among cascading FBG sensors leads to crosstalk. This issue poses a significant challenge in accurately discerning the specific central wavelength associated with each sensor. To address the challenge of crosstalk and the difficulty in discerning the central wavelength in cascading FBG sensors within IWDM systems, the implementation of machine learning-based algorithms for central wavelength interrogation has been proposed. This method is engineered to provide swift analytical abilities, improving the efficiency and precision of sensor wavelength detection, while the self-healing architecture further boosts system reliability by automatically correcting faults, ensuring continuous, robust operation even in challenging environments.

The primary thrust of this paper is the innovative integration of FBG sensors with FSO in a self-healing ring architecture. This integration is designed to augment the flexibility and resilience of the sensor system. An advanced technique for temperature sensing that utilizes the capabilities of FSO in conjunction with the precision of FBG sensors in a self-healing ring architecture is proposed. Furthermore, an unsupervised autoencoder (AE) mechanism within a convolutional neural network (CNN) model is implemented. This AE-CNN model specifically addresses the overlapping challenges of FBG sensors within IWDM systems. The findings suggest that this integrated approach, which synergizes self-healing architecture with cutting-edge machine learning techniques, represents a significant leap forward in sensor technology. It offers a solution that is not only more accurate and efficient, but also robust and adaptable for complex sensor system applications. The implications

of this research are far-reaching, promising transformative advancements for industries reliant on precise and reliable sensor technologies.

The remainder of this paper is structured as follows: Section 2 delves into the schematic diagram of the ring-based self-healing multi-channel architecture. Section 3 outlines the experimental setup, followed by Section 4, which describes the operational principle of the proposed system as well as the data collection method. This is then followed by Section 5, which introduces the proposed AE-CNN model. In Section 6, results and discussions are explained, and finally, Section 7 concludes the paper.

2. Schematic Diagram of the Ring-Based Self-Healing Multi-Channel Architecture

The proposed system, the FSO with an FBG sensor system in a self-healing ring architecture, is designed to enhance the precision and reliability of temperature sensing in critical environments such as gasoline storage areas, chemical storage facilities, and cement kilns. This integration is depicted in Figure 1, where the central office serves as the primary hub for distributing optical signals across various segments of the network through the FSO channel. The role of FSO is pivotal in ensuring high-speed data transmission and wireless connectivity, particularly in regions where traditional cabling is impractical. This wireless feature significantly enhances the system's resilience, enabling continuous communication even in the face of physical disruptions.

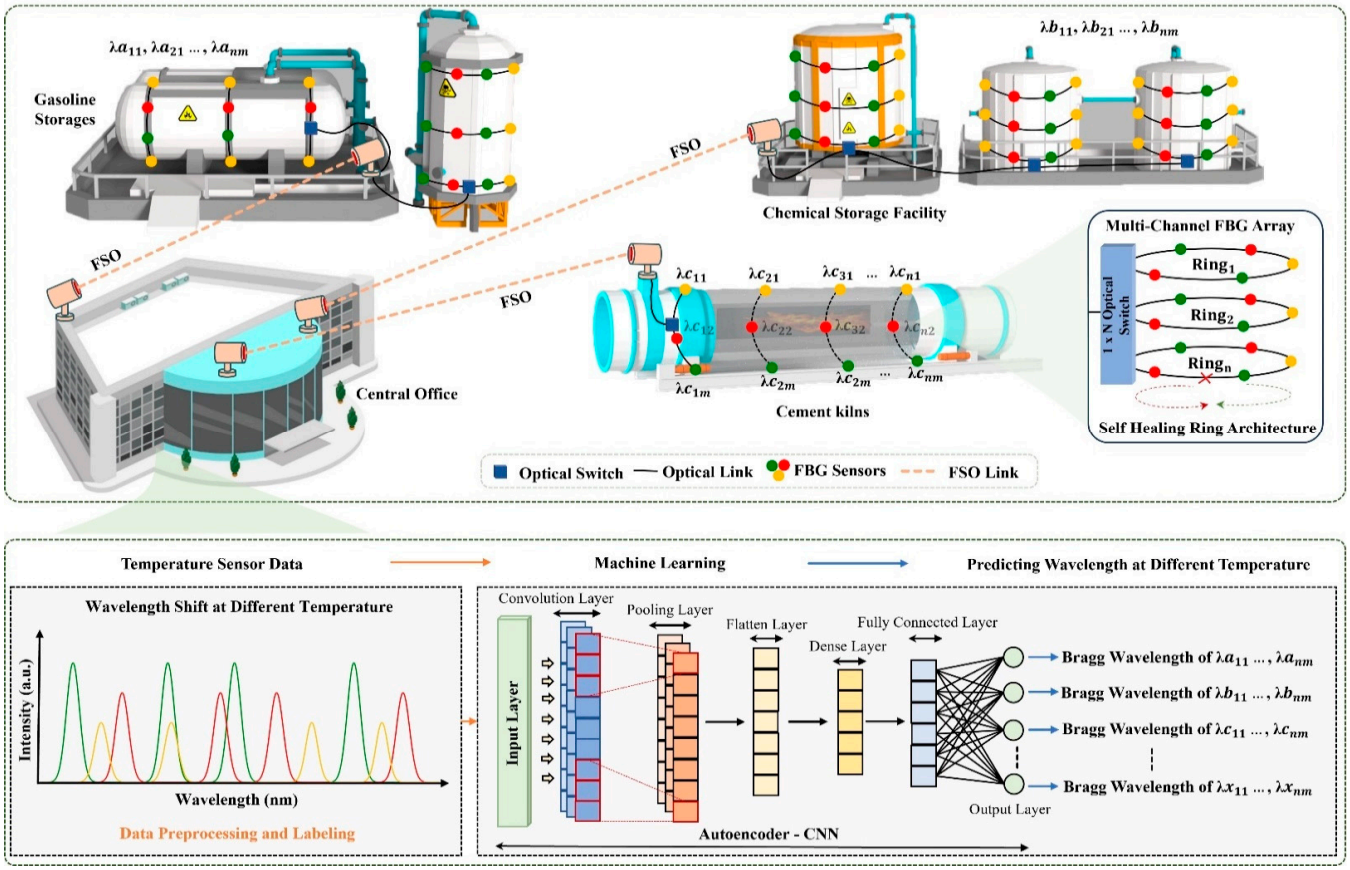

Figure 1. The schematic diagram of the proposed ring-based self-healing multi-channel FBG array architecture.

At each targeted location, the system utilizes a ring architecture composed of FBG sensors, arranged as λx_{nm} (where n represents the ring number and m represents the sensor count within that ring). These sensors are specifically designed to detect temperature changes by altering their reflection spectra in response to environmental variations. The reflected spectral data from the FBGs are recorded through an optical spectrum analyzer

(OSA) and subsequently processed for real-time monitoring. Furthermore, to address the issue of spectral overlap in FBG sensors, a deep learning approach that is specific to the AE-CNN model in the proposed system is proposed.

3. Experimental Setup

The experimental setup for the proposed study involves a self-healing architecture for an FBG sensor system, aimed at reducing the likelihood of system failures and enhancing robust connectivity. As illustrated in Figure 2, the system employs a ring-based self-healing design in conjunction with FSO, facilitating a strong and resilient system that can overcome physical obstacles. The incorporation of an optical switch within this architecture allows for dynamic reconfiguration and rerouting of signals in the event of a link breakdown [33–40]. This design choice significantly decreases the likelihood of sensor system failures and ensures continuous operation.

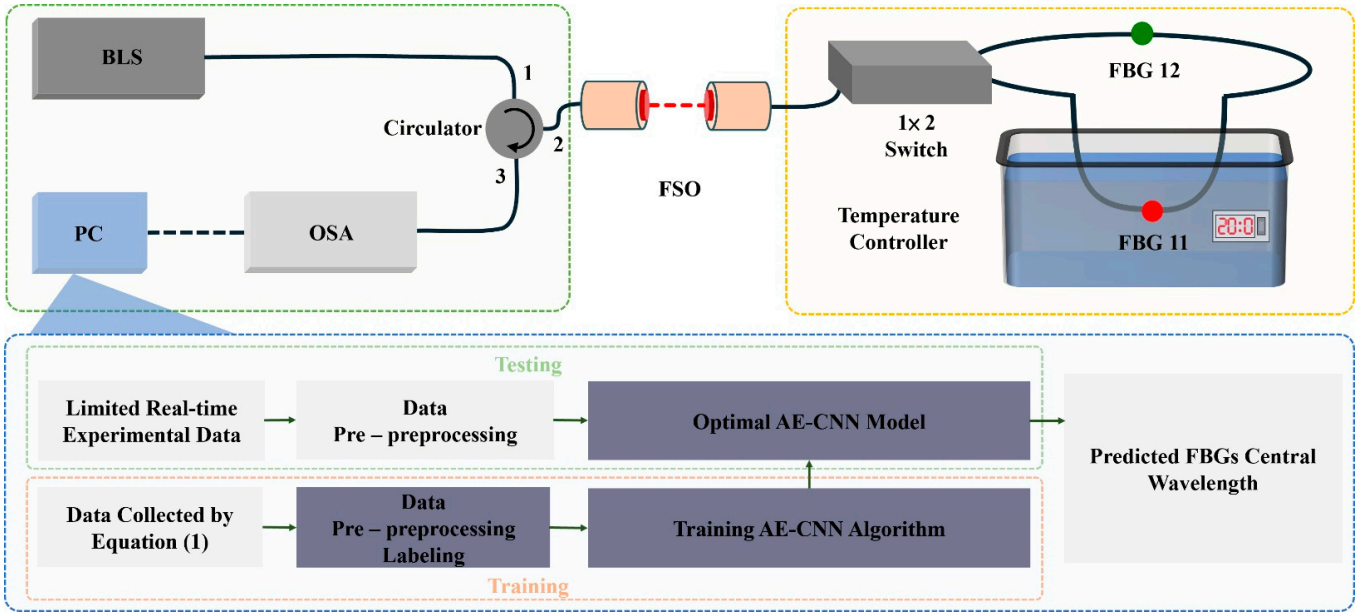

Figure 2. Experimental setup of proposed system with ring-based self-healing architecture FBG sensors system. BLS: broadband light source; OSA: optical spectrum analyzer; PC: personal computer; FSO: free-space optics.

The proposed experimental setup includes a broadband light source from which the signal is generated and then channeled into an optical circulator. The signal is then transmitted through the FSO channel to a 1 × 2 optical switch, directing it toward the FBG sensors. The setup comprises two FBG sensors, labeled FBG11 and FBG12. FBG11 is placed inside a temperature controller, while FBG12 is maintained at room temperature.

In the proposed systems, a wavelength shift occurs when strain and temperature are applied to a specific FBG sensor, as demonstrated in the experiment. This phenomenon of wavelength shift can also be induced by vibrations, such as those caused by environmental vibration and wind. However, the proposed experimental setup is meticulously designed and conducted in a controlled laboratory environment, thus mitigating external variables like wind-induced vibrations. This controlled environment allows for focused efforts on enhancing temperature measurement accuracy without external interference. Nonetheless, it is recognized that accounting for such factors in real-world applications is essential, with plans to address these challenges in future research.

4. Operational Principle of the Proposed System and Data Collection Method

In the proposed architecture devised for dataset collection, the design incorporates two distinct scenarios to comprehensively explore the capabilities of the system. Initially, in the first scenario, the dataset collection process is initiated with the deployment of two FBG sensors, and this configuration is demonstrated above in the experimental setup. This initial configuration serves as a foundational exploration, aiming to assess the basic functionality and performance of the system under controlled conditions. Moreover, due to the need for a more enhanced analysis and validation of the concept, a secondary scenario is introduced. In this expanded setup, the system is simulated to include six FBG sensors, representing a scenario with a more substantial sensor array. By augmenting the sensor count, the objective is to delve deeper into the intricacies of the system's behavior, capturing a richer dataset that can offer insights into its robustness, scalability, and potential limitations. This iterative approach enables a thorough investigation of the system's capabilities across varying sensor configurations, facilitating a more comprehensive understanding of its potential applications and informing future development efforts.

In the first scenario as shown in the proposed experimental setup, a controlled temperature is applied to FBG11, causing a shift in its central wavelength. The initial temperature of FBG11 is set at 25 °C and is gradually increased to 70 °C over 10 steps. On the other hand, FBG12 remains at a stable ambient temperature of 23 °C. The central wavelengths of FBG11 and FBG12 sensors are 1544.58 nm and 1544.59 nm, respectively. Each of the FBGs possesses a full-width at half maximum measuring 0.2 nm. During the experiment, the central wavelength of FBG11 changes from 1544.58 nm to 1545.05 nm over 10 temperature steps. The reflected wavelengths, captured by the OSA through the optical circulator, are then processed using a personal computer. The collected data exhibit an overlapping problem, as illustrated in Figure 3a, b, which complicates the interpretation and analysis. To effectively solve this issue, an AE-CNN deep learning approach is proposed to accurately predict the central wavelengths of the FBGs, thereby resolving the issue of overlapping.

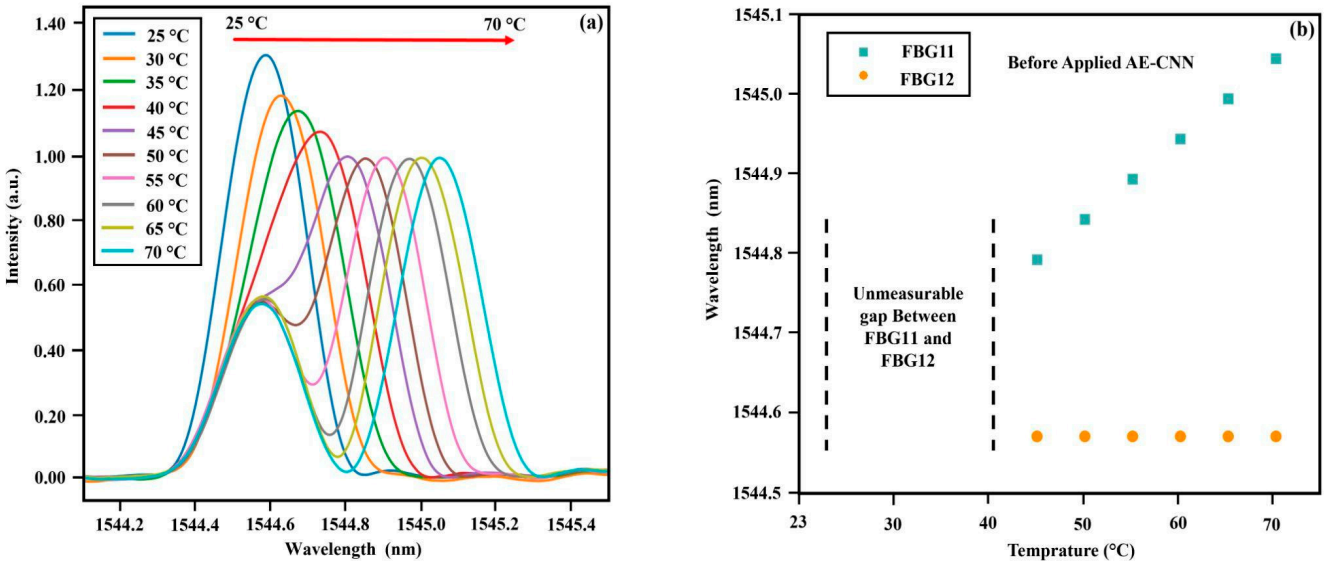

Figure 3. (**a**) Reflected spectra of two FBGs. (**b**) Unmeasurable spacing between FBG11 and FBG12.

In the second scenario depicted in the proposed schematic diagram, the focus is on highlighting the structure's versatility and adaptability for scaling up sensor integration in real-world applications. This structure also deals with its scalability and self-healing capabilities, emphasizing its ability to seamlessly integrate multiple sensors. By simulating scenarios with increased sensor counts, practical deployment conditions can be replicated to address diverse sensing needs efficiently. This examination assesses the structure's robustness in managing larger datasets and supporting various sensor types, validating

its flexibility across industries and applications for complex monitoring and analysis requirements. A crucial aspect of the FBG sensors is their reflection spectrum, which is assumed to originate from a single FBG with a Gaussian profile. The mathematical formulation [33] of the reflection spectrum is denoted by Equation (1):

$$R\left(\lambda, \lambda_{b,j}\right) = I_P \left[-4\, ln\, 2 \times \left(\frac{\lambda - \lambda_{b,j}}{\Delta\lambda_B}\right)^2\right] \quad (1)$$

In this equation, $\lambda_{b,j}$ is the central wavelength that depends on the measurement; I_P represents the intensity of the reflected peak; $\Delta\lambda_B$ symbolizes the full width at half maximum (FWHM) of the FBG; λ is the wavelength range; and $\lambda_{b,j}$ is the central wavelength of jth FBGs. Both I_P and $\Delta\lambda_B$ are crucial parameters in the designing of FBG sensor systems. Moreover, to prove the concepts and to evaluate the performance of the proposed model, even as the number of FBG sensors increases, simulation temperature data are collected from six FBG sensors, with which the model is trained and tested. Figure 4 illustrates computer-simulated spectral data for six FBGs with uniformly distributed central wavelengths ranging from 1542 nm to 1547 nm. When temperature is applied to FBG21, its central wavelength shifts from 1542.9 nm to 1547.9 nm over 25 temperature increments. The FBGs exhibit distinct peaks with varying power intensities, with FBG21 showing the highest intensity at 1.0 a.u., FBG22 at 0.8 a.u., FBG23 at 0.7 a.u., FBG24 at 0.6 a.u., FBG25 at 0.5 a.u., and FBG26 at 0.4 a.u.

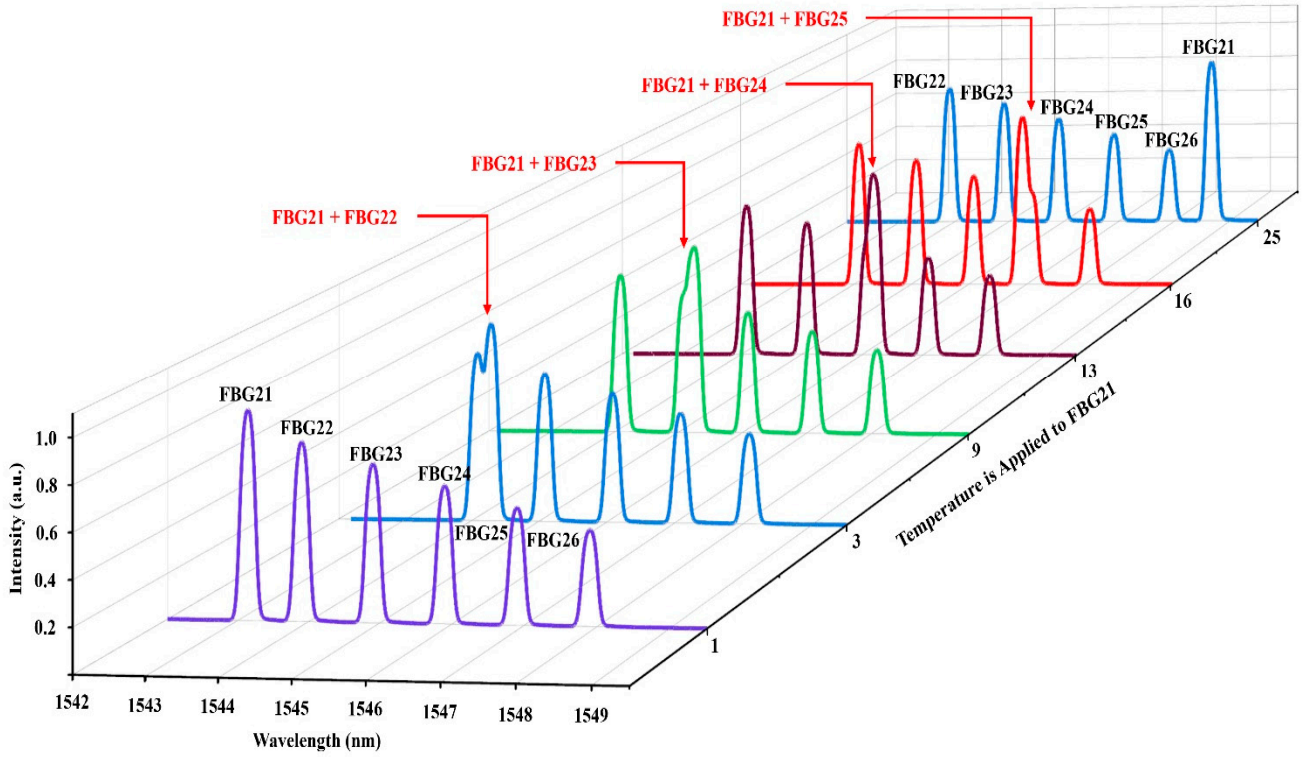

Figure 4. Spectral data for six FBGs generated through computer simulation.

To address the issue of spectral overlap in FBG sensors, the proposed system incorporates an AE-CNN model. This integration of the AE-CNN model is inspired by the need to improve the system's precision and effectiveness, especially in applications that demand accurate temperature measurements. The proposed model simplifies data processing and improves the accuracy of temperature sensing, thereby making the system more effective for real-world applications.

5. Proposed AE-CNN Model

The autoencoder convolutional neural network (AE-CNN) model, as depicted in Figure 1, stands as a cornerstone of the proposed system, addressing nonlinear regression challenges, particularly in the context of wavelength demodulation within FBG systems. The AE component of the model functions by compressing the input into a lower-dimensional latent space (encoding), acting as a form of dimensionality reduction. This process distills the essence of the data into a more manageable form, simplifying the regression task and making it more computationally efficient by focusing on the most relevant features. Additionally, the autoencoder can be pre-trained in an unsupervised manner, learning useful features before being fine-tuned for the specific regression task. The CNN part of the model leverages 1D convolutional layers to extract features from long-sequence spectral data. These layers use convolution kernels that travel through the input data along one spatial or temporal dimension, producing a tensor output for complex feature extraction. The AE-CNN's architecture comprises four encoder and decoder layers. The encoders include four sets of Conv1D operations paired with max-pooling, and the decoders consist of four sets of Conv1D operations complemented by upsampling. Conv1D excels in extracting features from the comprehensive time series of the sensor dataset. For training purposes, the proposed model utilized 1000 samples derived from Equation (1), with 1D spectral data, where wavelength ranges align with the array's indices. The training parameters included a batch size of 1000 and a learning rate set at 0.001. During the training, the Adam optimization method is adopted to minimize the inconsistency between the true central wavelength for each FBG and the model's predicted wavelength.

The configuration of the AE-CNN pre-trained system involves specifying the input shape as a tuple of integers (1, 1000), catering to sequences of N instances, each comprising a 1000-dimensional vector. The training process includes fine-tuning factors such as the number of epochs and batch size. Post-training, the system evaluates the input data spectrum and extracts the central wavelengths corresponding to each FBG. The extracted wavelengths are compared against the actual measured spectra, enabling the identification of discrepancies and facilitating continuous refinement in terms of accuracy through iterative processes. This cycle of training and improvement ensures a robust system capable of accurately determining the central wavelengths of FBGs. The max-pooling layer following each convolution operation reduces the data length: they are halved for the initial three layers and cut by a factor of five in the last layer. Conversely, the layer for increasing the sample resolution magnifies the input five-fold for the first layer and then reduces it by half for the subsequent three layers. To counteract potential gradient issues in deep architectures, an Exponential Linear Unit (ELU) activation function is incorporated between each successive layer, yielding faster training periods and heightened model accuracies compared to alternatives like the Rectified Linear Unit (ReLU). The architecture concludes with three densely connected layers with units set at 50, 25, and 5, respectively, all employing the ELU activation function.

After repetitively training the proposed model, the evaluation of its training performance is conducted using the training loss metric. As depicted in Figure 5, insights into the model's effectiveness in terms of training duration and the train loss of the AE-CNN model at different iterations are obtained. As depicted in the figure, the training loss gradually decreases as the training iterations increase.

Figure 6 demonstrates the training accuracy of the proposed AE-CNN model. As observed in Figures 5 and 6, the AE-CNN showcases commendable performance. The use of a limited training dataset allows for an in-depth analysis of the model's generalization capabilities under various testing conditions and data points. After 750 computational training cycles and weight initialization, the model is optimized.

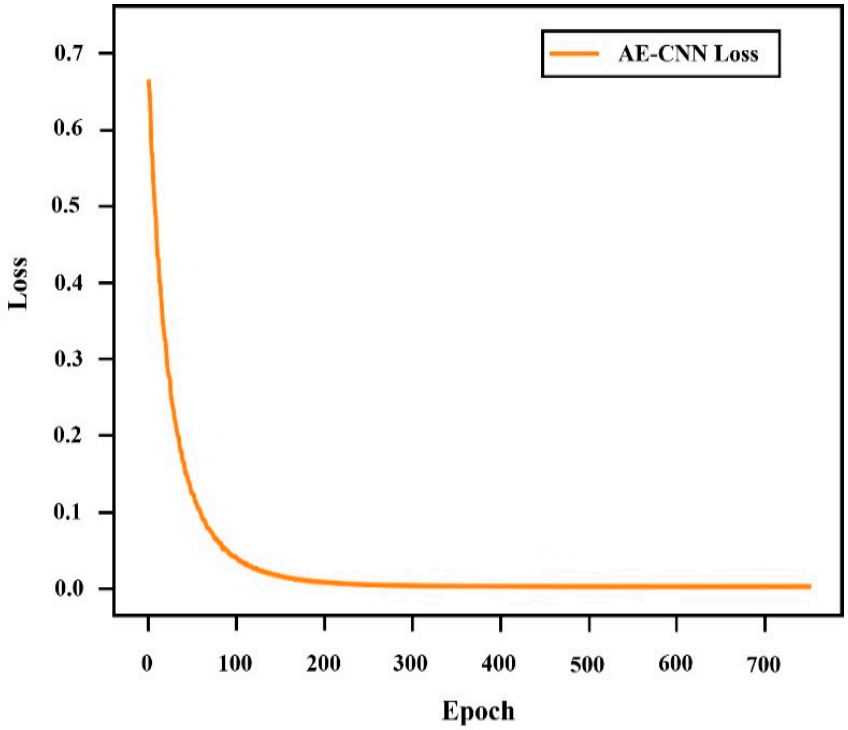

Figure 5. AE-CNN model's training loss across various iterations.

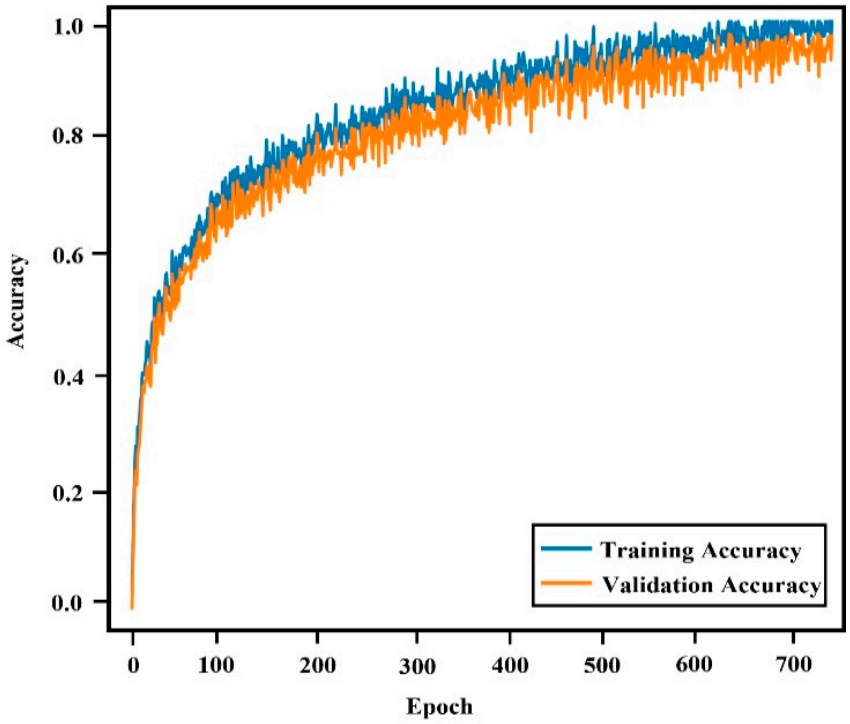

Figure 6. Training accuracy of the proposed AE-CNN model across various iterations.

6. Results and Discussion

The results of the proposed system are evaluated using two distinct scenarios. Initially, two FBG sensors are employed, and for a more thorough analysis, a second setup incorporating six FBG sensors is simulated. This approach guarantees a comprehensive evaluation from basic to more complex scenarios. In the first scenario, a single simplified ring subnetwork is used to demonstrate temperature measurement experimentally.

In the proposed experimental setup, FBG sensors are placed within a temperature controller. When temperature is applied to a specific FBG sensor, this causes a shift in its central wavelength. These shifts in central wavelengths create signal overlaps, resulting in crosstalk among the cascaded sensors. Particularly, Figure 3a displays the reflected spectral data samples from two FBGs at varying temperature steps. Overlapping spectra in FBGs lead to crosstalk, significantly reducing the sensor system's efficiency. Consequently, these issues make it difficult to differentiate each sensor's response using traditional peak wavelength detection methods. To tackle this overlap issue, the model is fed with the comprehensive long sequence spectrum, enabling the extraction of Bragg wavelengths from the intertwined FBG spectra. Therefore, the AE-CNN model has been proposed to address these issues. By utilizing this model, the issue of overlapping spectra, including the specific case of the unmeasurable gap highlighted in Figure 3a, is successfully resolved. The AE-CNN model demonstrates the ability to efficiently identify and precisely predict the peak wavelengths of overlapping FBG sensors. The proposed method's results show the detected Bragg wavelengths for each FBG across different temperatures and stages, including scenarios with complete overlap, as seen in Figure 7. This capability ensures that previously unmeasurable gaps can be accurately measured and analyzed with a high degree of precision.

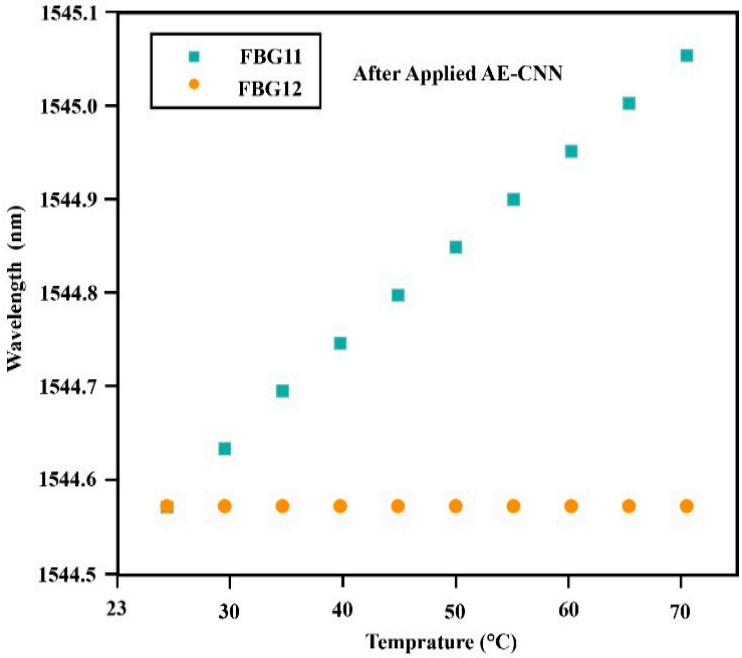

Figure 7. The peak wavelengths of two FBGs detected using the proposed AE-CNN.

To evaluate the accuracy of Bragg wavelength detection, the root-mean-squared error (RMSE) method is employed [31]. The RMSE is defined in Equation (2):

$$\text{RMSE} = \sqrt{\frac{\sum_{i=1}^{n}(y_i - y)^2}{n}} \tag{2}$$

The count of forecasted values, the actual value, and the forecasted value are denoted by the letters n, y_i, and y, respectively. RMSE in the first scenario is noted to be 0.035. The second scenario aims to verify the system's effectiveness with an increased number of sensors.

As shown in Figure 7, the unmeasurable gap problem between two FBGs shown in Figure 3b is solved after applying the proposed AE-CNN, which means that the proposed model accurately detects the peak wavelength of each FBG even if the spectra of two FBGs are fully overlapped. The AE-CNN model is not only a powerful tool for overcoming the

overlapping problem in FBG sensors, as evidenced by the data in Figure 7, but also exemplifies state-of-the-art advancements in sensor technology. Its combination of autoencoder capabilities for feature learning and dimensionality reduction, along with the convolutional neural network's proficiency in feature extraction and regression, makes it an ideal choice for intricate tasks like wavelength demodulation in FBG systems. This model signifies a remarkable advancement in the capacity to analyze and interpret complex sensor data.

From the experimental setup, it is reasonable to infer that the proposed solution can handle the overlapping of sensors like FBG11, FBG12, and others, under various temperature conditions. This is evident from its ability to resolve overlaps when temperature is applied to different sensors, as the overlapping spectra result from the combined output intensities of each stressed FBG. In this paper, we specifically showcase the scenario where temperature is applied to FBG11, demonstrating the effective measurement of the Bragg wavelength for each FBG. The proposed system's capability to discern each FBG's Bragg wavelength under temperature, as seen when applied to FBG11, assures its functionality even when temperature is applied to FBG12 or other sensors. This research utilizes an AE-CNN model, especially when working with a dataset comprising 30,000 training and 6000 testing data points. The AE-CNN model excels in processing complex datasets, efficiently interpreting nonlinear relationships within the data.

In the proposed system, to demonstrate the concept, the initial temperature of a specific FBG sensor is set within the range of 25 °C to 70 °C. In this context, FBG sensors designed to operate across a wide temperature range exhibit versatility in their functionality [7,8]. FBG sensors are capable of measuring temperatures beyond the specified range in the proposed systems, as demonstrated in numerous applications [7,8]. The proposed AE-CNN model can also effectively determine the overlapping spectral data, and is capable of accurate temperature detection across the entire operational range of FBG sensors, even at temperatures lower than 45 °C. This solution ensures that the proposed system can effectively influence the wide temperature range of FBG sensors, overcoming spectral overlapping issues. This enhancement increases the system's relevance and reliability in real-world situations.

In many practical contexts, issues frequently intensify as the quantity of training samples and the complexity of features both escalate simultaneously. Particularly in the proposed system, as the number of connected sensors increases, there will be an increase in spectral overlap and complexity. Within these dynamic conditions, deep learning models frequently emerge as robust solutions, demonstrating their exceptional performance capabilities. Deep learning algorithms excel with extensive and diverse training data, proficiently interpreting complex patterns in real-world scenarios.

Hence, this paper proposes the integration of unsupervised autoencoders (AEs) with convolutional neural networks (CNNs) to address the sequential problem in scenarios with a significant amount of spectral overlapped data and complexity. This fusion results in superior performance, establishing its essentiality across various domains. In this paper, a simplified experiment was conducted using a small number of FBG sensors to demonstrate the proof of concept. Consequently, an experimental evaluation was performed to verify that the proposed system can measure a large number of overlapping spectra while strain is applied to multiple sensors simultaneously. The autoencoder component efficiently reduces dimensionality and extracts relevant features from complex and overlapping spectral data. Subsequently, the CNN component refines these features to improve the prediction accuracy of individual FBG sensor readings. As mentioned above, when strain is applied to certain sensors, the proposed hybrid AE-CNN model can predict the central wavelength of each FBG even when the spectra of two or three FBGs are overlapped simultaneously.

Figure 8 highlights the output of the second scenario, emphasizing that the system's assessment of each FBG's central wavelength remains precise even with an increased sensor count or in a complex FBG sensor system. The RMSE for this scenario is 0.124.

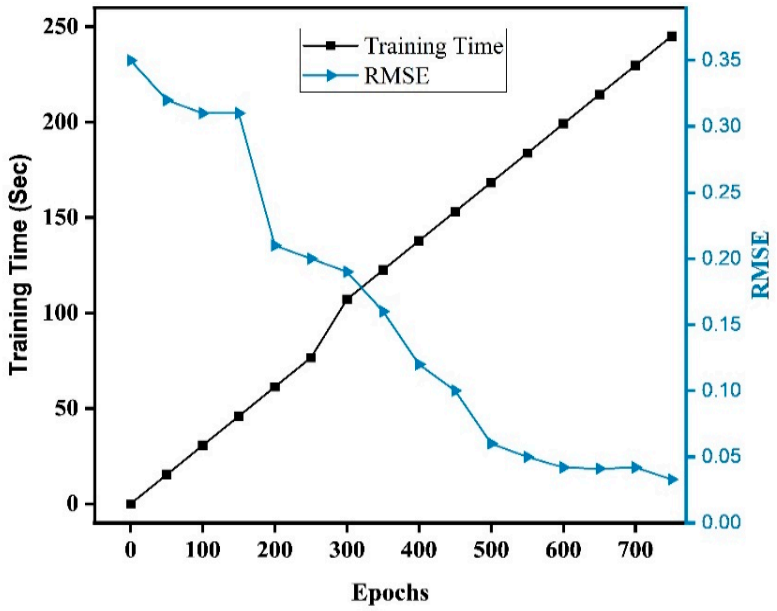

Figure 8. Effectiveness of the model evaluated by training duration and the root-mean-squared error across various iterations.

Its sophisticated architecture, merging CNNs' pattern recognition with autoencoders' processing efficiency, significantly enhances its performance. Additionally, the model's training time efficiency, as detailed in Figure 8, is complemented by the computer-simulated spectrum shown in Figure 8, while Figure 9 displays the results of the simulation, showing detected wavelengths when temperature is applied to FBG21. These results further validate the effectiveness of the proposed system in accurately determining wavelengths under varying conditions, demonstrating its robustness and reliability in practical applications.

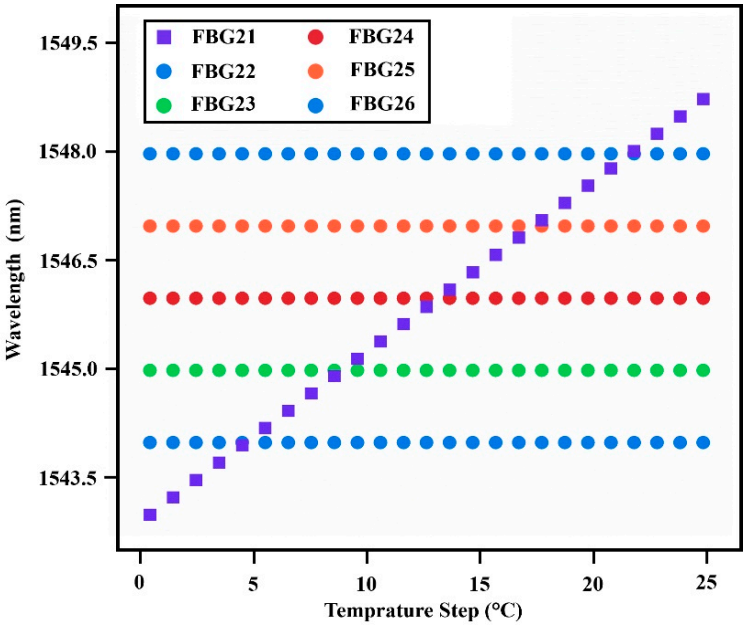

Figure 9. The detected wavelengths when temperature is applied to FBG21.

Generally, in the proposed system, an initial experimental setup with two FBG sensors is followed by a demonstration of the system's scalability in practical applications through a simulation involving six FBG sensors to prove the concept. In both scenarios, the proposed AE-CNN model is capable of detecting spectral overlap and improving temperature

measurement accuracy. The design of the AE-CNN model inherently facilitates scalability, allowing for efficient handling of large spectral datasets and analysis from numerous FBG sensors. This scalability is crucial for real-world applications involving extensive sensor networks. The findings of the proposed system indicate that the model maintains its performance in terms of accuracy and reliability even with an increasing number of sensors, highlighting its suitability for large-scale deployments.

In the examination of the AE-CNN model's performance, particularly in its application to FBG sensor systems, a nuanced comparison with preceding methodologies reveals its distinctive advantages. This work, through the deployment of AE-CNN, manifests a pivotal improvement in the precision of Bragg wavelength detection under varied temperature conditions, as evidenced by the root-mean-squared error (RMSE) metric. The AE-CNN model's RMSE signifies not only a leap in accuracy, but also underscores the model's effectiveness in interpreting complex spectral data.

Further, when delving into the attributes beyond RMSE, this work differentiates itself with the integration of full-spectrum optimization FSO and self-healing capabilities. These features are particularly salient when juxtaposed with other referenced methods such as the neural networks (NNs) and sparse autoencoders (SAEs) from [20], extreme learning machines (ELMs) from [31], and differential evolution (DE) from [41]. The inclusion of FSO in this work allows for a more comprehensive analysis of the spectral data, ensuring that no significant information is lost during the process. This is in contrast to the methods that may not fully exploit the entirety of the available data spectrum, potentially overlooking critical insights.

Moreover, the self-healing capability embedded within the AE-CNN framework marks a significant advancement in the resilience of sensor systems. This attribute ensures that the system can maintain operational efficacy and quickly recover from any disruptions, a feature not explicitly afforded by the methodologies in [20,30,31,41]. This work's emphasis on self-healing is indicative of an understanding of the dynamic challenges faced in practical applications, where sensor systems must be robust against a variety of unpredictable conditions.

This discussion, by focusing on the specific achievements and the unique features of the AE-CNN model, provides a clear perspective on its standing in the context of FBG sensor analysis. Without making overarching statements or promises, it can be observed that the specific advancements introduced in this work, particularly in terms of RMSE performance, FSO, and self-healing capabilities, present a meaningful contribution to the field. These enhancements not only improve the accuracy and reliability of temperature and spectral analyses, but also augment the resilience and adaptability of the sensor systems, marking a significant stride in the domain.

7. Conclusions

In summary, the fusion of FBG sensors with FSO within ring-based self-healing architectures presents a promising horizon for sensor technology. FBG sensors, renowned for their sensitivity and durability, are invaluable in challenging environments such as aerospace and structural health monitoring. Their synergy with FSO elevates signal quality, bolsters reliability, and reduces latency in expansive sensor systems, while the self-healing feature enhances system resilience, enabling automatic adjustments to maintain optimal performance. Addressing the intricacies of multiplexing FBG sensors, this study introduced a groundbreaking intensity and wavelength division multiplexing (IWDM) approach. To alleviate the issue of overlapping FBG spectra, innovative unsupervised autoencoder convolutional neural network (AE-CNN) mechanisms are implemented, resulting in significant enhancements in system accuracy, computational efficiency, and setup simplicity. In essence, this research signifies a substantial stride toward seamlessly integrating FBG sensors with FSO technology, ushering in the potential for more robust and efficient sensor systems. These advancements hold the promise of transforming data acquisition and analysis in demanding environments, particularly benefiting sectors such as aerospace,

structural health monitoring, and various scientific and industrial fields. This study unveils a promising and dependable future for sensor technology.

Author Contributions: Conceptualization, M.A.A. and P.-C.P.; methodology, M.A.A., C.-K.Y., C.-H.P., Y.C.M. and P.-C.P.; software and data preparation, M.A.A. and C.-K.Y.; model validation, M.A.A.; formal analysis, M.A.A., A.M.D., Y.C.M., S.T.H., C.-K.Y., C.-H.P., P.K. and P.-C.P.; investigation, M.A.A., A.M.D., Y.C.M., S.T.H., C.-K.Y., C.-H.P., P.K. and P.-C.P.; writing—review and editing, M.A.A., A.M.D., Y.C.M., S.T.H. and P.-C.P. All authors have read and agreed to the published version of the manuscript.

Funding: This work was supported by the National Science and Technology Council, Taiwan, under Grant NSTC 112-2221-E-027-076-MY2.

Institutional Review Board Statement: Not applicable.

Informed Consent Statement: Not applicable.

Data Availability Statement: Dataset available on request from the authors.

Conflicts of Interest: The authors declare no conflicts of interest.

References

1. Pan, Y.; Liu, T.; Jiang, J.; Liu, K.; Wang, S.; Yin, J.; He, P.; Yan, J. Simultaneous Measurement of Temperature and Strain Using Spheroidal-Cavity-Overlapped FBG. *IEEE Photonics J.* **2015**, *7*, 1–6.
2. Liu, N.; Li, Y.; Wang, Y.; Wang, H.; Liang, W.; Lu, P. Bending Insensitive Sensors for Strain and Temperature Measurements with Bragg Gratings in Bragg Fibers. *Opt. Express* **2011**, *19*, 13880–13891. [CrossRef] [PubMed]
3. Aashia, R.; Madhav, K.; Srinivasan, B.; Asokan, S. Strain-Temperature Discrimination Using a Single Fiber Bragg Grating. *IEEE Photonics Technol. Lett.* **2010**, *22*, 778–780. [CrossRef]
4. Ashry, I.; Mao, Y.; Trichili, A.; Wang, B.; Ng, T.K.; Alouini, M.S.; Ooi, B.S. A Review of Using Few-Mode Fibers for Optical Sensing. *IEEE Access* **2020**, *8*, 179592–179605. [CrossRef]
5. Kersey, A.D.; Davis, M.A.; Patrick, H.J.; LeBlanc, M.; Koo, K.P.; Askins, C.G.; Putnam, M.A.; Friebele, E.J. Fiber Grating Sensors. *J. Light. Technol.* **1997**, *15*, 1442–1463. [CrossRef]
6. Al-Fakih, E.; Osman, N.; Adikan, F.R.M. The Use of Fiber Bragg Grating Sensors in Biomechanics and Rehabilitation Applications: The State-of-the-Art and Ongoing Research Topics. *Sensors* **2012**, *12*, 12890–12926. [CrossRef]
7. Ma, S.; Xu, Y.; Pang, Y.; Zhao, X.; Li, Y.; Qin, Z.; Liu, Z.; Lu, P.; Bao, X. Optical Fiber Sensors for High-Temperature Monitoring: A Review. *Sensors* **2022**, *22*, 5722. [CrossRef] [PubMed]
8. Laffont, G.; Cotillard, R.; Roussel, N.; Desmarchelier, R.; Rougeault, S. Temperature Resistant Fiber Bragg Gratings for On-Line and Structural Health Monitoring of the Next-Generation of Nuclear Reactors. *Sensors* **2018**, *18*, 1791. [CrossRef]
9. Mihailov, S.J. Fiber Bragg Grating Sensors for Harsh Environments. *Sensors* **2012**, *12*, 1898–1918. [CrossRef]
10. Ghosh, C.; Priye, V. Augmentation of Sensitivity of FBG Strain Sensor for Biomedical Operation. *Appl. Opt.* **2018**, *57*, 6906–6910. [CrossRef]
11. Tosi, D. Review and Analysis of Peak Tracking Techniques for Fiber Bragg Grating Sensors. *Sensors* **2017**, *17*, 2368. [CrossRef] [PubMed]
12. Hu, Y.; Mo, W.; Dong, K.; Jin, F.; Song, J. Using Maximum Spectrum of Continuous Wavelet Transform for Demodulation of an Overlapped Spectrum in a Fiber Bragg Grating Sensor Network. *Appl. Opt.* **2016**, *55*, 4670–4675. [CrossRef] [PubMed]
13. Zhang, W.; Zhang, M.; Lan, Y.; Zhao, Y.; Dai, W. Detection of Crack Locations in Aluminum Alloy Structures Using FBG Sensors. *Sensors* **2020**, *20*, 347. [CrossRef] [PubMed]
14. Colpo, F.; Humbert, L.; Botsis, J. An Experimental Numerical Study of the Response of a Long Fiber Bragg Grating Sensor Near a Crack Tip. *Smart Mater. Struct.* **2007**, *16*, 1423–1432. [CrossRef]
15. Fang, L.; Chen, T.; Li, R.; Liu, S. Application of Embedded Fiber Bragg Grating (FBG) Sensors in Monitoring Health to 3D Printing Structures. *IEEE Sens. J.* **2016**, *16*, 6604–6610. [CrossRef]
16. Takahashi, N.; Yoshimura, K.; Takahashi, S. Detection of Ultrasonic Mechanical Vibration of a Solid Using Fiber Bragg Grating. *Jpn. J. Appl. Phys.* **2000**, *39*, 3134. [CrossRef]
17. Kumar, P.; Shih, G.-L.; Yao, C.-K.; Hayle, S.T.; Manie, Y.C.; Peng, P.-C. Intelligent Vibration Monitoring System for Smart Industry Utilizing Optical Fiber Sensor Combined with Machine Learning. *Electronics* **2023**, *12*, 4302. [CrossRef]
18. Ghosh, C.; Priye, V. Highly Sensitive FBG Strain Sensor with Enhanced Measurement Range Based on Higher Order FWM. *IEEE Photonics J.* **2020**, *12*, 1–7. [CrossRef]
19. Yao, K.; Lin, Q.; Jiang, Z.; Zhao, N.; Peng, G.-D.; Tian, B.; Jia, W.; Yang, P. Design and Analysis of a Combined Strain–Vibration–Temperature Sensor with Two Fiber Bragg Gratings and a Trapezoidal Beam. *Sensors* **2019**, *19*, 3571. [CrossRef]
20. Manie, Y.C.; Yao, C.-K.; Yeh, T.-Y.; Teng, Y.-C.; Peng, P.-C. Laser-Based Optical Wireless Communications for Internet of Things (IoT) Application. *IEEE Internet Things J.* **2022**, *9*, 24466–24476. [CrossRef]

21. Naik, R.P.; Simha, G.D.G.; Krishnan, P. Wireless-Optical-Communication-Based Cooperative IoT and IoUT System for Ocean Monitoring Applications. *Appl. Opt.* **2021**, *60*, 9067–9073. [CrossRef] [PubMed]
22. Killinger, D. Free Space Optics for Laser Communication Through the Air. Opt. *Photonics News* **2002**, *13*, 36–42. [CrossRef]
23. Bloom, S.; Korevaar, E.; Schuster, J.; Willebrand, H. Understanding the Performance of Free-Space Optics. *J. Opt. Netw.* **2003**, *2*, 178–200. [CrossRef]
24. Sadiku, M.; Musa, S.; Nelatury, S. Free Space Optical Communications: An Overview. *Eur. Sci. J. ESJ* **2016**, *12*, 55. [CrossRef]
25. Harres, D. Military Aircraft Fiber Optics Networks: Status & Direction. *IEEE Aerosp. Electron. Syst. Mag.* **2004**, *19*, 16–22.
26. Leitgeb, E.; Plank, T.; Pezzei, P.; Ivanov, H.; Jiménez, R.P. Optical Wireless Communications and Optical Sensing and Detection Technologies for Increasing the Reliability and Safety in Autonomous Driving Scenarios. In Proceedings of the 20th International Conference on Transparent Optical Networks (ICTON), Bucharest, Romania, 1–5 July 2018; pp. 1–4.
27. Yu, Y.-L.; Liaw, S.-K.; Chou, H.-H.; Le-Minh, H.; Ghassemlooy, Z. A Hybrid Optical Fiber and FSO System for Bidirectional Communications Used in Bridges. *IEEE Photonics J.* **2015**, *7*, 7905509. [CrossRef]
28. Abdul Sattar, S.M.; Saleh, M.A.; Abass, A.; Ali, M.; Yaseen, M. Bidirectional Hybrid Optical Communication System Based on Wavelength Division Multiplexing for Outdoor Applications. *Opt. Quantum Electron.* **2021**, *53*, 597. [CrossRef]
29. Boukerche, A.; Sun, P. Connectivity and Coverage Based Protocols for Wireless Sensor Networks. *Ad Hoc Netw.* **2018**, *80*, 54–69. [CrossRef]
30. Manie, Y.C.; Peng, P.-C.; Shiu, R.-K.; Hsu, Y.-T.; Chen, Y.-Y.; Shao, G.-M.; Chiu, J. Enhancement of the Multiplexing Capacity and Measurement Accuracy of FBG Sensor System Using IWDM Technique and Deep Learning Algorithm. *J. Light. Technol.* **2020**, *38*, 1589–1603. [CrossRef]
31. Manie, Y.C.; Shiu, R.-K.; Peng, P.-C.; Guo, B.-Y.; Bitew, M.A.; Tang, W.-C.; Lu, H.-K. Intensity and Wavelength Division Multiplexing FBG Sensor System Using a Raman Amplifier and Extreme Learning Machine. *J. Sens.* **2018**, *2018*, 7323149. [CrossRef]
32. Zhang, L.; Liu, Y.; Williams, J.A.R.; Bennion, I. Enhanced FBG Strain Sensing Multiplexing Capacity Using Combination of Intensity and Wavelength Dual-Coding Technique. *IEEE Photonics Technol. Lett.* **1999**, *11*, 1638–1640. [CrossRef]
33. Chan, C.C.; Jin, W.; Demokan, M.S. Enhancement of Measurement Accuracy in Fiber Bragg Grating Sensors by Using Digital Signal Processing. *Opt. Laser Technol.* **1999**, *31*, 299–307. [CrossRef]
34. Takada, A.; Park, J.H. Architecture of Ultrafast Optical Packet Switching Ring Network. *J. Light. Technol.* **2002**, *20*, 2306. [CrossRef]
35. Gu, H.W.; Chang, C.H.; Chen, Y.C.; Peng, P.C.; Kuo, S.T.; Lu, H.H.; Li, C.Y.; Yang, S.S.; Jhang, J.J. Hexagonal Mesh Architecture for Large-Area Multipoint Fiber Sensor System. *IEEE Photonics Technol. Lett.* **2014**, *26*, 1878–1881. [CrossRef]
36. Feng, K.M.; Wu, C.Y.; Yan, J.H.; Lin, C.Y.; Peng, P.C. Fiber Bragg Grating-Based Three-Dimensional Multipoint Ring-Mesh Sensing System with Robust Self-Healing Function. *IEEE J. Sel. Top. Quantum Electron.* **2012**, *18*, 1613–1620. [CrossRef]
37. Yeh, C.; Xie, Y.-R.; Luo, C.-M.; Chow, C. Integration of FSO Traffic in Ring-Topology Bidirectional Fiber Access Network with Fault Protection. *IEEE Commun. Lett.* **2020**, *24*, 589–592. [CrossRef]
38. Sun, X.; Chan, C.-K.; Wang, Z.; Lin, C.; Chen, L.-K. A Single-Fiber Bi-Directional WDM Self-Healing Ring Network with Bi-Directional OADM for Metro-Access Applications. *IEEE J. Sel. Areas Commun.* **2007**, *25*, 18–24. [CrossRef]
39. Yeh, C.; Hsu, W.; Wang, B.-Y.; You, W.-Y.; Chen, J.-R.; Chow, C.; Liaw, S. Fiber- and FSO-Protected Connections for Long-Reach TWDM Access Architecture with Fault Protection. *IEEE Access* **2020**, *8*, 189982–189988. [CrossRef]
40. Hayle, S.T.; Manie, Y.C.; Dehnaw, A.M.; Hsu, Y.-T.; Li, J.-W.; Liang, H.-C.; Peng, P.-C. Reliable Self-Healing FBG Sensor Network for Improvement of Multipoint Strain Sensing. *Opt. Commun.* **2021**, *499*, 127286. [CrossRef]
41. Liu, D.; Tang, K.; Yang, Z.; Liu, D. A Fiber Bragg Grating Sensor Network Using an Improved Differential Evolution Algorithm. *IEEE Photonics Technol. Lett.* **2011**, *23*, 1385–1387. [CrossRef]